Lawrence Berkeley National Laboratory
Recent Work

Title
RECOIL PROPERTIES OF FISSION PRODUCTS

Permalink
https://escholarship.org/uc/item/6gw5c204

Authors
Alexander, John M.
Gazdik, M. Frances.

Publication Date
1960-03-01

UNIVERSITY OF CALIFORNIA

Ernest O. Lawrence

Radiation

Laboratory

BERKELEY, CALIFORNIA

DISCLAIMER

UNIVERSITY OF CALIFORNIA

Lawrence Radiation Laboratory
Berkeley, California

Contract No. W-7405-eng-48

RECOIL PROPERTIES OF FISSION PRODUCTS

John M. Alexander and M. Frances Gazdik

March 1960

RECOIL PROPERTIES OF FISSION PRODUCTS

John M. Alexander and M. Frances Gazdik

Lawrence Radiation Laboratory
University of California
Berkeley, California

March 1960

ABSTRACT

The range and relative rates of energy loss in Al and Au have been measured radiochemically for five products from thermal-neutron-induced fission of U^{235}. Range-velocity relationships for the median light product of fission and the median heavy product have been obtained from these measurements and other workers' energy-loss data. The relation of range (R) to energy (E) or velocity (V) can be fitted to functions of the form $R = kV-\Delta$ or $R = KE^{2/3}$. We have assumed that these functional forms can be applied to fission products of any mass. The constants K and Δ were determined from values of the range and kinetic energy for products of high yield. The values of these constants have been extrapolated to products of low yield. We have estimated kinetic energies, heretofore unmeasured, from the ranges of low-yield products.

We have interpreted certain radiochemical observations in terms of the average component of the range perpendicular to the original velocity. The value of this component in Au has been estimated to be about one-fifth the total range.

for the latter type of experiment. However, the interpretation of these experiments requires information about the form of the angular distribution and the nature of the stopping process.

From the measurements reported here and elsewhere[15,16] we have constructed curves of the range in Al and Au as a function of the mass number of the recoiling fission product. These curves define quite accurately the ranges of the median light and heavy products. (By "median product" is meant that fragment that is the median of all the light fission products or all the heavy fission products.) We normalize the available energy-loss data for median light and heavy products to the range values. This combination of information provides range-velocity curves for the median light and heavy products. Similar curves are proposed for all fission products. Finally, we estimate the kinetic energies of products of low yield from their range.

EXPERIMENTAL PROCEDURE

We have made radiochemical measurements of the range of Sr^{89}, Ag^{111}, Cd^{115}, I^{131}, and Ba^{140} from thermal-neutron fission of U^{235} by the thin-target-thick-catcher technique originated by Douthett and Templeton.[1] The target diagram is shown in Fig. 1. A thin layer of U^{235} was sprayed on 0.00025-in. Al foil.[17] The mass of U^{235} per unit area was determined by measuring the alpha radiation per unit area. The target and several catcher foils (Al and Au) were stacked as shown in Fig. 1, and clamped between two pieces of cardboard. The target assembly was irradiated in the thermal column of the LPTR reactor at Livermore for several days with a flux of about 5×10^{11} neutrons/cm^2 sec.

Recoil catcher foils

| Guard | Blank | 3A | 2A | 1A | 1B | 2B | 3B | 4B | Blank | Guard |

U^{235} layer
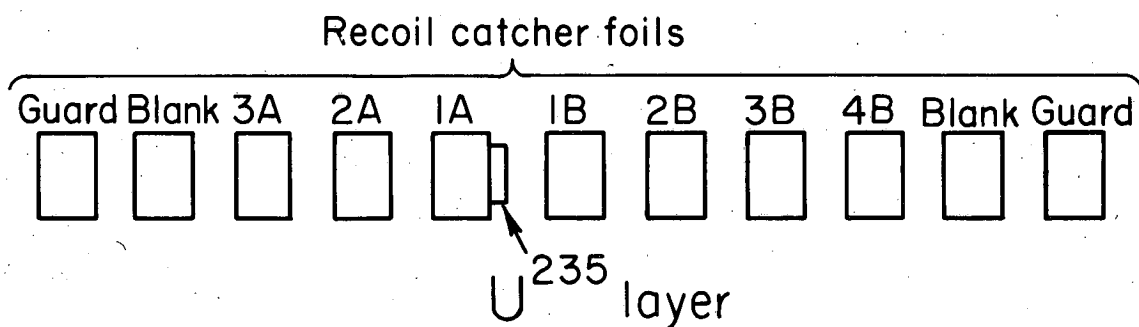
MU — 19554

Fig. 1. Diagram of the foil stack. A thin layer of
fissile material was supported on the surface of
catcher 1A. Space between the foils is only for
clarity of the drawing; during the irradiation the
foils were in contact. In Tables I and III are
given the types and thicknesses of the catcher foils.

Commercially rolled Al (99.5% Al) foils of about 0.00025 inch were wiped with a lint-free tissue and cut into squares of 10.26 cm^2 in area with a stainless steel template. A very smooth central region of about 36 $in.^2$ was found in all Al sheets. All squares cut from this central region of a given Al sheet had weights uniform within at least 0.5%. Commercially available Au foil was not so uniform, and therefore more uniform Au foils were prepared by evaporation. Commercial Au foil was used for all catchers except 1B (Fig. 1) because the thickness of these foils was not critical for the range measurement.

After irradiation, the foils were separated and dissolved in HCl and H_2O_2. The target layer was included with the catcher designated 1A. Iodine carrier was always present during the dissolution if iodine was to be separated. Standard radiochemical procedures were used.[18] Chemical yields were determined by weighing before counting and checked by another analysis after counting. These two analyses had an average deviation of about 1%. Counting was done with β proportional counters or with an integral γ counter. All samples of the same element from a given experiment were counted simultaneously on several β counters in rotating fashion, in order to determine the relative activities as accurately as possible. The chemical yields were so similar (usually constant to 10%) that counting-efficiency corrections were in general negligible. The γ radiation from I^{131} and Ba^{140} were also counted on a NaI scintillation detector sensitive to all photons with energy greater than about 60 kev.

ANALYSIS OF EXPERIMENTAL RESULTS

In this section a number of experimental observations are presented. In Part A the observations are used to deduce range values in Al, and the effect of the target layer is discussed. In Part B evidence is presented which

indicates that the recoil paths of the products in Au deviate considerably from a straight line. Range values in Au are obtained with certain assumptions concerning the nature of the scattering. Finally, in Part C we report experimental quantities pertinent to the relative stopping power of Al and Au.

A. Range Measurements in Al

The experimental observations for those experiments in which only Al catchers were used are presented in Table I. Column 1 gives the fission product studied, and column 2 the experiment number. Columns 3-8 give for each catcher foil the designation, the thickness, and the fraction of the total atoms in question that stopped in that foil. The last column gives the mass of U^{235} per unit area of the fissile layer.

In these experiments the fissile nucleus is essentially at rest and the angular distribution of the products is isotropic. Let F_t denote the fraction of the recoils of a specific product that pass through a catcher of thickness t from a thin target of thickness W. Then

$$F_t = \frac{1}{2} \left(1 - \frac{t}{R} - \frac{cW}{2R} \right),$$ (1)

where $1/R$ denotes the average reciprocal range of the product in the catching foil. The derivation of this equation (see Appendix) requires the approximation that the rate of velocity loss in the target layer, $-\left(\frac{dV}{dx}\right)$, be proportional to the rate of velocity loss in the catcher foil, $\left(\frac{dV}{dR}\right)$:

$$-\frac{dV}{dx} = c \frac{dV}{dR}.$$ (2)

Table I. Experiments with Al catchers.
Fraction of activity observed for the various catchers

| Fission product | Expt. no. | Catchers Number, substance, thickness (mg/cm²) | | | | | | (mg/cm²) U²³⁵ in the target |
		3A Al 1.92	2A Al 1.92	1A+tgt. Al 1.923	1B Al 1.923	2B Al 1.92	3B Al 1.92	
Sr^{91}	1	0.0264	0.2287	0.2501	0.2396	0.2318	0.0234	0.062
Sr^{89}	2	0.0215	0.2378	0.2400	0.2414	a	a	0.122
Ag^{111}	3		0.2264	0.2816	0.2739	0.2181		0.045
Ag^{111}	2		0.2083	0.2908	0.2873	0.2136		0.122
Ag^{111}	4		0.1882	0.3258	0.2971	0.1888		0.368
I^{131}	3		0.2099	0.2849	0.2915	0.2139		0.045
I^{131}	2		0.1990	0.3060	0.2983	0.1967		0.122
I^{131}	4		0.1779	0.3344	0.3128	0.1750		0.368
Ba^{140}	1		0.1703	0.3349	0.3284	0.1665		0.062
Ba^{140}	2		0.1602	0.3437	0.3342	0.1617		0.122

[a]These samples were lost; therefore the total activity was obtained with the

assumption 2A+3A = 2B+3B.

This is possibly not a good approximation for those recoils which are appreciably slowed down in the target. Therefore only F_t values with $t \gg cW$ have been used to deduce range values.

In order to obtain range values from the observed quantities given in Table I, the value of c must be determined. From Eq. (1) it is clear that

$$\left(\frac{\partial F_t}{\partial W}\right)_t = -\frac{c}{4R} \, . \tag{3}$$

The value of $\left(\frac{\partial F_t}{\partial W}\right)_t$ was determined for Ba^{140}, I^{131}, and Ag^{111} by a least-squares fit to the data of Table I (see Fig. 2). Values of c and R for these products were obtained from Eqs. (1) and (3). The values of c that resulted were essentially the same for these three products. Thus the assumption is made that c is independent of fission product and the average value of 1.4_7 (mg of Al/mg of U^{235} in the target) was used for all range determinations.

The composition of the target layer is expected to be U_3O_8. A crude estimate of c may be made with the assumption that $\frac{dV}{dR} \alpha M^{-1/2}$ (cm^3/mg sec) where M denotes the mass number of the stopping material. The value of c so estimated is about 1/2 (mg of Al/mg of U^{235} in the target); this is about one-third the observed value. A similar effect was observed by Douthett and Templeton, who suggested that inhomogeneities in the target layer might increase the effective target thickness.[1] The presence of water molecules or foreign matter in the target would also tend to increase the magnitude of c, but it is difficult to explain this large difference between the estimated and observed values.

The observations in Table I have been analyzed by means of Eq. (1) to give ranges in Al. The ranges are listed in Table II. The first column gives the
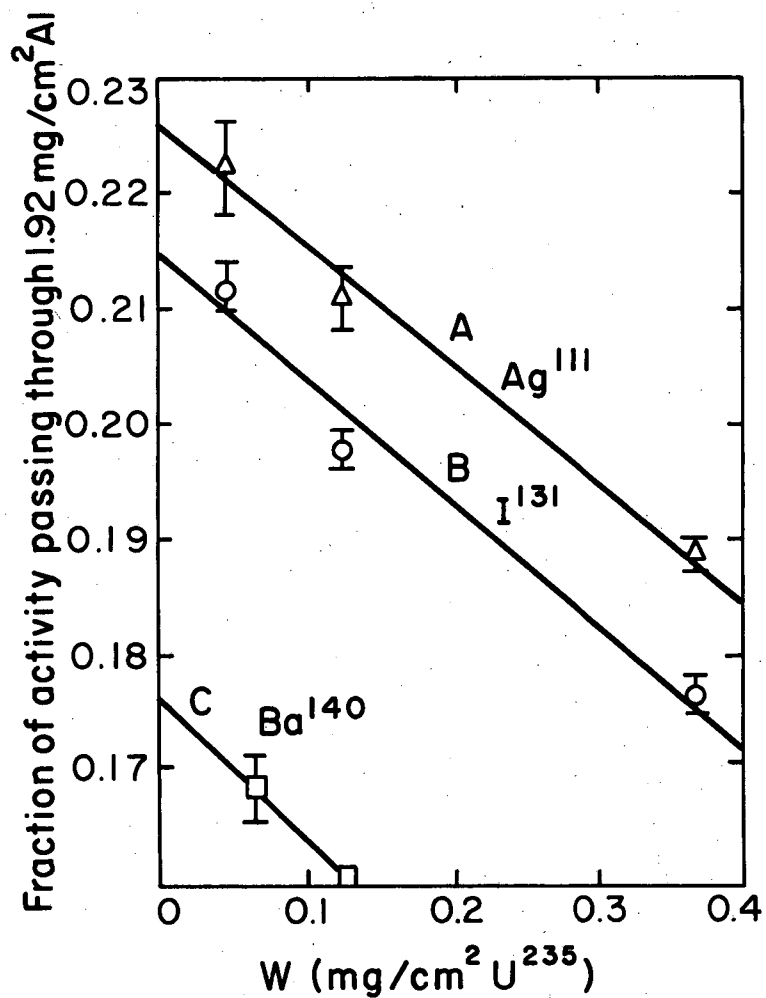
MU-19555

Fig. 2. Least-squares fit to linear dependence of F_t on
W, the mass of U^{235} per unit area of the target
layer. The ratio   of initial rate of velocity loss
in the target to that in Al was determined for
Ag^{111}, I^{131}, and Ba^{140}.

A: Ag^{111}_{131}: c = 1.5 (least squares)
B: I^{131}_{140}: c = 1.4 (least squares)
C: Ba^{140}: c = 1.5

fission product and the last the experiment number. Columns 2-4 give the range

values resulting from the fraction of the total activity observed in the catcher

or catchers designated.

B. Range Measurements in Au and the Problem of Scattering

The experimental observations for those experiments in which both Al and

Au catcher foils were used are presented in Table III. Column 1 gives the

particular fission product observed. Columns 2-8 give the designation of each

catcher foils, its thickness and type, and the fraction of the total activity

observed in that foil. Column 9 gives an estimate of the fraction of the

activity retained by the target layer, F_W, namely

$$F_W = cW/2R. \tag{4}$$

If Eq. (1) is a good approximation for $t = 0$, Eq. (4) should give a good

approximation to F_W.

From the data in Table I we can evaluate F_W for Experiments 1-4 by sub-

tracting the fraction observed in Catcher 1B from that in 1A plus target. In

general, these measured values of F_W are less than $cW/2R$. There is poor re-

producibility of the ratio of F_W to $cW/2R$, which may be due to diffusion or

scattering effects or "rub-off" of some of the target layer on the 1B foil.

In any case Eq. (4) certainly gives an upper limit to the activity retained by

the target. The target layers were so thin in Experiments 5-8 that uncertain-

ties in F_W are not very important in the range determinations.

If each fission product traveled along a straight path we would expect the

sum of the fractions observed in the A foils to be one-half the total activity

increased by $1/2 F_W$. However, from the first nine columns in Table III we note

Table II. Results of experiments with Al catchers.
Range values(mg/cm^2 Al) calculated from the F_t values observed in various catchers[a]

| Fission product | Catchers | | | | Experiment number |
	3A	2A+3A	2B+3B	3B	
Sr^{91}	$\lesssim 4.11$[b]	4.02	4.02	$\lesssim 4.08$[b]	1
Sr^{89}	$\lesssim 4.11$[b]	4.18			2
Ag^{111}		3.57	3.47		3
Ag^{111}		3.45	3.51		2
Ag^{111}		3.52	3.52		4
I^{131}		3.37	3.42		3
I^{131}		3.34	3.32		2
I^{131}		3.40	3.37		4
Ba^{140}		2.99	2.95		1
Ba^{140}		2.96	2.98		2

[a] These values were calculated from Eq. (1),

$$R = \frac{t + \frac{cW}{2}}{1 - 2F_t} \, ,$$

taking $c = 1.4_7$ (mg of Al/mg of U^{235}) for all cases.

[b] The values from catchers 3A and 3B of Experiment 1 were omitted in calculating the average range because of possible violation of the straggling requirement. In Experiment 2 experimental errors were evidently greater than the straggling perturbation.

Table III. Experiments with Au and Al catchers.
Fraction of activity observed in the various catchers

Catcher, thickness (mg/cm^2), substance

Experiment 5

Fission product	3A 1.626 Al	2A 1.626 Al	1A+tgt. 1.626 Al	1B[a] 4.876 Au	2B 1.056 Al	3B 1.036 Al	4B 1.002 Al	Target[b] 0.035 U235	F_b[c] Fraction backscattered
Sr89	.1020	.2110	.2258	.1645	.1466	.1278	.0224	.0062	.0357
Ag111 d	.0384	.2263	.2662		.1444	.0973	<.002	.0073	.0272
Cd115 d	.0200	.2320	.2715		.1518	.0787	<.002	.0077	.0196
I131 d	.0218	.2331	.2824		.1559	.0834	<.002	.0076	.0335
Ba140	<.002	.2261	.3074	.2556	.1611	.0496	<.0004	.0086	.0292

Experiment 6

Fission product	3A 1.626 Al	2A 1.626 Al	1A+tgt. 1.626 Al	1B 4.953 Au	2B 1.053 Al	3B 1.044 Al	4B 1.031 Al	Target 0.017 U235	F_b Fraction backscattered
Sr89	.1026	.2008	.2301	.1700	.1463	.1300	.0203	.0030	.0320
Ag111 d	.0377	.2288	.2633		.1483	.0989	e	.0035	.0281
I131 d	.0213	.2355	.2834		.1524	.0837	<.0004	.0037	.0385
Ba140	<.0006	.2250	.3117	.2583	.1588	.0462	<.0001	.0042	.0346

Experiment 7

Fission product	3A 1.628 Al	2A 1.628 Al	1A+tgt. 1.625 Al	1B plus 2B 1.986 Au / 1.650 Al	3B 1.650 Al	Target .011 U235	F_b Fraction backscattered
Sr89	.1032	.1940	.2209	.2778	.2042	.0020	.0171
Cd115	.0211	.2321	.2785	.3398	.1285	.0024	.0305
Ba140	.0024	.2233	.3023	.3698	.1021	.0027	.0266

Experiment 8

Fission product	3A 4.622 Au	2A 4.717 Au	1A+tgt. 1.626 Al	1B 4.971 Au	2B 4.970 Au	3B 4.758 Au	Target .015 U235	F_b Fraction backscattered
Ba140	.0055	.2147	.3135	.2690	.1961	.0013	.0037	.0319

Table III (cont'd.)

[a]The Au foil was prepared by evaporation, its uniformity checked by cutting small squares from various parts of the foil. Activation of impurities in the Au was checked in Experiments 7 and 8, and found to be negligible.

[b]The activity retained in the target was taken to be $(cW/2R_{Al})$ from the data in Table V and $c = 1.4_7$ (mg of Al/mg of U^{235}). The range values are not very sensitive to this correction because the targets were quite thin.

[c]The fraction of the total activity in the A foils in excess of one-half plus $1/2\ F_W$ was attributed to backscattering from the Au. The quantity F_b is defined as the net fraction backscattered. F_b = sum of fractions in foils designated by A - $1/2\ F_W$ - $1/2$.

[d]No observation was made of 1B in these cases. The total activity was calculated from the activity observed in catchers 2A+3A and the average range value reported in Table V (see Eq. (1)).

[e]Some activity of long half life was observed in this foil, which prevented setting a limit on the Ag^{111} activity.

that in each case the foils designated by A have a larger fraction of the total activity than one-half plus $1/2\ F_W$. We attribute this excess activity to backscattering from the Au into the Al, and designate the net fraction backscattered by F_b. The values of F_b are given in the final column of Table III.

Bohr has presented a qualitative theory of the stopping of fission frag-ments.[19] The theory predicts that the major mechanism of energy loss at the end of the range is nuclear collisions, whereas the initial energy degradation is mainly by ionization. In the ionization region very small angular deflections and small range straggling are expected. However, in the nuclear-stopping region, larger deflections and the major contribution to the range straggling are expected. Fission-fragment tracks in photographic emulsions[20] and cloud chambers[21] bear out the theory with respect to angular deflections. The recoiling product is thus expected to move straight initially and to suffer deflections as it approaches the end of the range. Let us define the vectors $\vec{p}$ as the average component of range along the original direction of motion and $\vec{q}$ as the average component of the range perpendicular to the original direction of motion. We assume that the effect is as if each fission product recoils a distance $\vec{p}$ and then moves a distance $\vec{q}$. (See the Appendix.)

Equation (1) does not take account of the angular deflection. This effect can be included by allowing $\vec{q}$ to be equally probable at all azimuthal angles. In the Appendix we derive the relations

$$F_b \simeq \frac{1}{2\pi} \left[\left(\frac{q}{R}\right)_{Au} - \left(\frac{q}{R}\right)_{Al} \right], \tag{5}$$

$$_{Al}F_{Au} \simeq \frac{1}{2} - \frac{1}{2}\left(\frac{t'}{p}\right)_{Au} + F_b \left[1 - \frac{1}{2}\left(\frac{t'}{R}\right)^2 - \frac{1}{8}\left(\frac{t'}{R}\right)^4\right]_{Au} + \frac{1}{8}\left(\frac{t'}{p}\right)\left(\frac{q}{R}\right)^2_{Au} , \quad (6)$$

where $_{Al}F_{Au}$ denotes the fraction of the activity passing through an Au catcher

of thickness t into an Al catcher, and t' is the effective catcher thickness,

$t + \frac{cW}{2}$.

The derivation of Eq. (5) does not require the assumption that the recoil

path coincides with $\vec{p}$ and $\vec{q}$. Only the effect of recoils crossing the interface

more than once has been ignored. However, Eq. (6) depends on the assumptions

that the recoil path coincides with $\vec{p}$ and $\vec{q}$ on the average and that $q_{Au} \gg q_{Al}$.

The error due to these approximations is difficult to evaluate, but is not expected

to be large.

Equations (1), (5), and (6) have been used to analyze the experimental ob-

servations in Table III, and the results of this analysis are presented in Table

IV. The first two columns of Table IV give the particular fission product and

the experiment number. Column 3 gives the range in Al from Eq. (1); column 4

gives the quantity $\left(\frac{q}{R}\right)_{Au} - \left(\frac{q}{R}\right)_{Al}$ from Eq. (5); and column 5 gives the range in

Au from experiments 5 and 6 using Eq. (6), and from experiment 8 using Eq. (1).

The values of $\left|(q/R)_{Au} - (q/R)_{Al}\right|$ estimated from Eq. (5) and the measured

quantity F_b are quite large. In addition to the F_b values from experiments 5

and 6 there are two other experimental observations consistent with large values

of $(q/R)_{Au}$. The first is the F_b value of 0.017, observed for Sr^{89} in experiment

7, compared with 0.034 in experiments 5 and 6. The thickness of the Au catcher

(1B) in experiment 7 was less than q_{Au} for Sr^{89}, which was estimated from Eq.

(5) and experiments 5 and 6. Thus from this analysis of the scattering a lower

F_b is expected for Sr^{89} in experiment 7. Secondly, the activity of Sr^{89} than that

observed in catcher 2A of experiments 5, 6, and 7 is slightly greater than that

Table IV. Results of experiments with Al and Au catchers

Fission product	Experiment number	R_{Al} (mg/cm^2)	$\left(\frac{q}{R}\right)_{Au} - \left(\frac{q}{R}\right)_{Al}$	R_{Au} [c] (mg/cm^2)
Sr^{89}	5	4.12 [a]	0.22	10.7
Sr^{89}	6	4.11 [a]	0.20	10.8
Sr^{89}	7	4.11 [a]		
Ag^{111}	5		0.17	8.8
Ag^{111}	6		0.18	9.1
Cd^{115}	5	3.36 [b]	0.12	8.6
Cd^{115}	7	3.31	0.19	
I^{131}	5		0.21	8.6
I^{131}	6		0.24	8.6
Ba^{140}	5	3.01	0.18	7.9
Ba^{140}	6	2.98	0.22	7.9
Ba^{140}	7	2.98	0.17	
Ba^{140}	8		0.20	8.26

[a] These values were calculated from the fraction of activity observed in 3A (See Table III). Ranges for Sr^{89} calculated from the fraction in 2A were about 3% smaller; this is attributed to backscattered recoils. This effect is assumed to be negligible for the other products.

[b] This value was calculated from the ratio of the fraction in 3A to the fraction in 2A relative to I^{131}. Straggling effects were assumed to be identical.

[c] The scattering correction was made (see Eqs. (5) and (6)) by using the average value of F_b and the assumption $q_{Au} \gg q_{Al}$.

expected from the range in Al deduced from all the other observations. This

is probably due to a very small contribution from recoils scattered in the Au

catcher (1B) which have enough energy to pass through catcher 1A.

In a completely different experimental arrangement Coffin and Halpern

have observed a group of recoiling fission products with about one-fifth the

usual range.[8] They interpreted this finding as due to recoiling products

scattered in their target layer. This result also indicates that large

angular deflections are important in the stopping process, and, in fact,

suggests a value of about one-fifth for (q/R) in their target material.

We have evaluated the range in Au with the assumption that $q_{Au} \gg q_{Al}$

(Eq. (6)). These range values should probably be considered lower limits

because if q_{Al} is not negligible with respect to q_{Au} the range values obtained

from Eq. (25) (see the Appendix) are larger than those listed. For example, if

$(q/R)_{Au} = 5 (q/R)_{Al}$ the range values (from Eq. (25)) are about 5% greater than

those obtained from Eq. (6). The measurement of the range of Ba^{140} in

experiment 8 compared to experiments 5 and 6 gives an estimate of the error

due to this effect. The range value for Ba^{140} as determined from experiment 8

and Eq. (1) is about 3% greater than the values from experiments 5 and 6 and

Eq. (6). Therefore we estimate that errors in R_{Au} from Eq. (6) are about -1%

to +4%.

The average range values determined in this work are given in Table V.

The number of products studied in this work and in earlier experiments elsewhere

is certainly not very large. However, it is possible to construct a somewhat

fragmentary range-mass curve. The ratios of range values reported by Finkle

and co-workers[16] are much more accurate than the absolute values. We have

Table V. Average range values

Fission product	Range in Al (mg/cm^2)	Range in Au (mg/cm^2)	R_{Al}/R_{Au}
Sr^{89}	4.12 ± 0.02[a]	10.8[a]	0.382
Sr^{91}	4.02		
Ag^{111}	3.51 ± 0.02	9.0	0.390
Cd^{115}	3.33 ± 0.04	8.6	0.387
I^{131}	3.37 ± 0.02	8.6	0.392
Ba^{140}	2.98 ± 0.01	8.0	0.373

[a]The quoted errors are the standard deviation of the mean. The ranges in Au probably have systematic errors of about -1% to +4% because of scattering phenomena.

therefore normalized those measurements to ours and have drawn a smooth curve

in Fig. 3. This curve allows a fairly accurate interpolation to mass numbers

near those of the products studied in this work. We consider that the range of

the median light and heavy fission products can be taken from this curve with

an accuracy of approximately 1.5%. Also in Fig. 3 we have shown the kinetic

energy data as a function of mass number of the fission product.[12]

The ratio of range in Al to range in Au appears to be slightly dependent

on the mass of the product, as shown in Fig. 4.

C. Relative Stopping Effectiveness of Au and Al

From the radiochemical data one can evaluate the ratio of range in Al to

range in Au and the relative rates of velocity loss in Al and Au. Let us de-

note by F_{Au+Al} the fraction of the recoils of a given product which pass through

both an Au foil (of thickness t_{Au}) and an Al foil (of thickness t_{Al}). If the

fission products are emitted isotropically, as is the case in these experiments,

we have

$$F_{Au+Al} = 1/2(1 - \cos \Theta_{max}). \qquad (7)$$

The Θ_{max} value derived from this measurement of F_{Au+Al} represents the angle

made by a fission product that penetrates a thickness of Au given by

$T_{Au} \equiv t_{Au}/\cos \Theta_{max}$ and has a residual range in Al given by $RR_{Al} \equiv t_{Al}/\cos \Theta_{max}$.

Thus a thickness of Au given by t_{Au} has a stopping effect equivalent to a thick-

ness of Al given by $R_{Al} - RR_{Al}$. Also a product that has a residual range in Al

of RR_{Al} would have a residual range in Au of $R_{Au} - T_{Au}$.

In Table VI we have listed the measured quantities pertinent to relative

stopping effectiveness of Al and Au. The first two columns give the fission
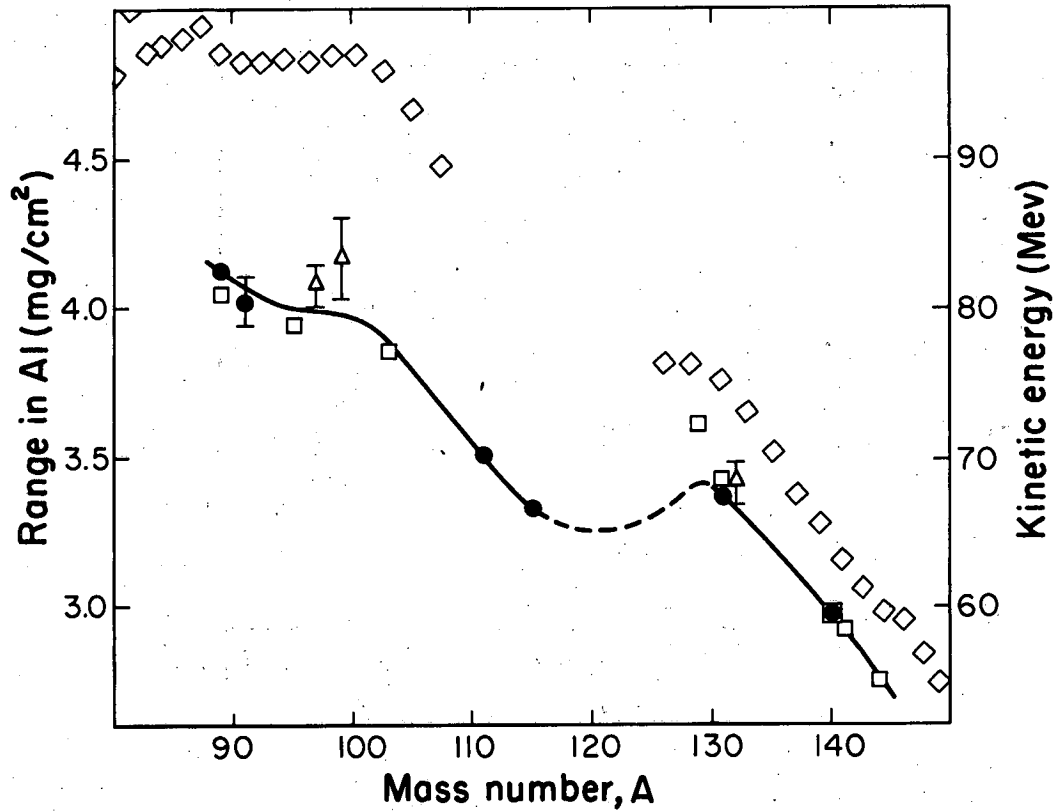
MU – 19556

Fig. 3.   Range in Al and kinetic energy of products from
     fission of U235 induced by thermal-neutron irradia-
     tion.   The experimental range values are designated
     as follows: The circles from this work; the triangles
     from reference 15; and the squares from reference 16,
     normalized to these results by the factor 1.084.
     The diamonds show the kinetic energy of the products
     as taken from reference 12.
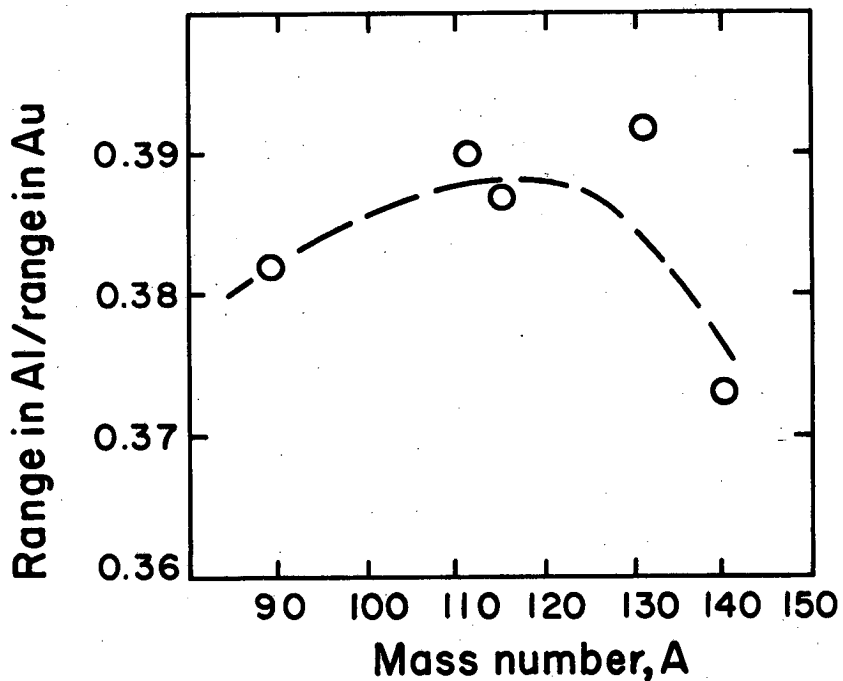
MU-19557

Fig. 4.   The ratio of range in Al to range in Au. The
          limits of error for these ratios are about -4% to
          +1%.   These errors are largely systematic, there-
          fore the dependence on A believed to be more
          accurate.

product and experiment number. Columns 3 and 4 give the measured quantities T_{Au} and RR_{Al}. In the last column is given the velocity corresponding to the value of RR_{Al}. This velocity was estimated from the empirical range-velocity parameters for Al that are presented in the next section (Eq. (8) and Fig. 14).

From the data given in Tables V and VI we can sketch the velocity dependence of the ratio of range in Al to range in Au $(RR_{Al}/(R_{Au} - T_{Au})$ or R_{Al}/R_{Au}. This dependence is plotted in Fig. 5. That velocity was taken which corresponds to the value of RR_{Al}. Similar behavior for all products is indicated in Fig. 5. As the velocity is decreased to about 0.7 (Mev/nucleon)$^{1/2}$ the ratio of range in Al to range in Au seems to be almost constant. Further decrease in the velocity results in a sharp increase in this ratio. Further decrease in the velocity results in a sharp increase in this ratio. Also included in Fig. 5 are two values[22] of R_{Al}/R_{Au} for At^{203}. The velocity of the At^{203} atoms is much less than that of the fission products reported in this work, but the range ratio is quite consistent with the trend of these values.

Another way of comparing the stopping in Al and Au is to sketch the ratio of the quantity $\Delta V/\Delta R$ for Al to that for Au as a function of velocity. These ratios are shown in Fig. 6. From the values of R, T, and RR we have calculated the thickness of Al which is equivalent to a certain thickness of Au. For instance, in the initial degradation a thickness $R_{Al} - RR_{Al}$ is equivalent to T_{Au}. If two measurements of T_{Au} and RR_{Al} were made, then a thickness of Al given by the difference of RR_{Al} values is equivalent to a thickness of Au given by the difference of T_{Au} values. For simplicity we have plotted these ratios of Al thickness to equivalent Au thickness $\left[(\Delta V/\Delta R)_{Au}/(\Delta V/\Delta R)_{Al} \right]$ at a velocity which is the average of the velocity at entrance and the final velocity in the

Table VI. Quantities pertinent to relative stopping power of Au and Al

Fission product	Experiment number	T_{Au} $(mg/cm^2)Au$	RR_{Al} $(mg/cm^2)Al$	$V(RR_{Al})$[a] $(Mev/nucleon)^{1/2}$
Sr^{89}	5	7.08	1.51	0.723
Sr^{89}	6	7.14	1.51	0.723
Sr^{89}	7	3.40	2.79	1.093
Ag^{111}	5	6.15	1.31	0.563
Ag^{111}	6	6.22	1.31	0.563
Cd^{115}	5	5.88	1.25	0.539
Cd^{115}	7	2.71	2.22	0.804
I^{131}	5	5.95	1.27	0.484
I^{131}	6	5.99	1.26	0.481
Ba^{140}	5	5.50	1.17	0.458
Ba^{140}	6	5.50	1.16	0.455
Ba^{140}	7	2.53	2.07	0.708

[a]The velocities corresponding to RR_{Al} were taken from Eq. (8) and Fig. 14.
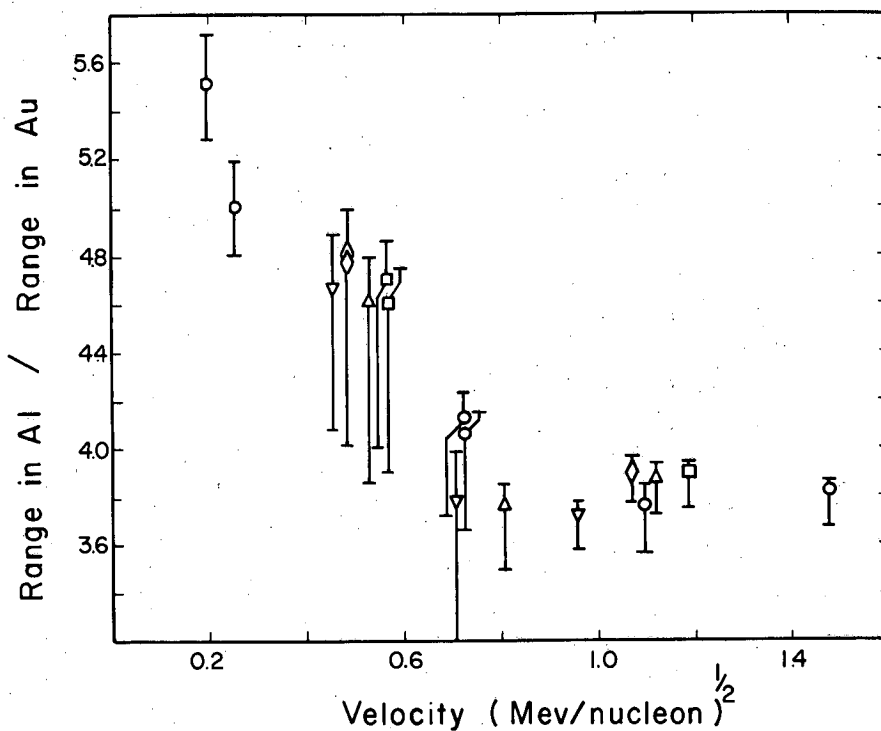
MU — 19558

Fig. 5. Velocity dependence of the ratio of range in Al to range in Au. The symbols are as follows: Sr[89] $\bigcirc$; Ag[111] $\square$; Cd[115] $\triangle$; I[131] $\diamond$; Ba[140] $\triangledown$; At[203] $\blacklozenge$. The At[203] measurements are from Ref. 22. The error estimates are mainly from uncertainties in R_{Au} which are systematic.
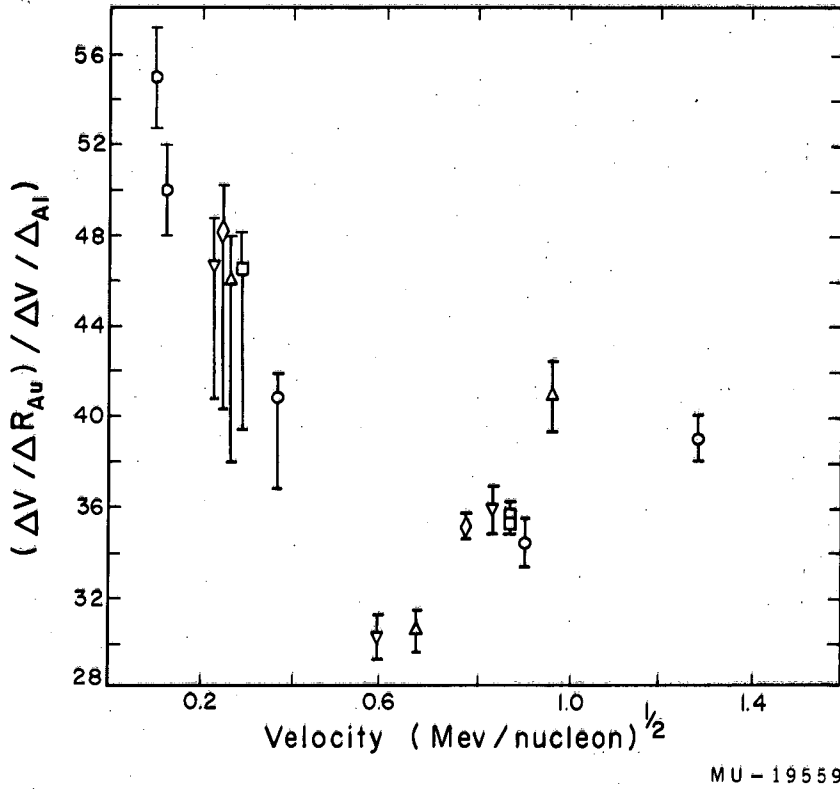
MU-19559

Fig. 6. Velocity dependence of the ratio of the rate
of velocity (or energy) loss in Au to that in

Al $[(\frac{\Delta V}{\Delta R})_{Au} / (\frac{\Delta V}{\Delta R})_{Al}]$.

The symbols are as follows: Sr[89] O ; Ag[111] ▢ ;
Cd[115] △ ; I[131] ◇ ; Ba[140] ▽ ; At[203] ◗. The
At[203] measurements are from reference 22.

region in question. For example, the ratio R_{Al}-RR_{Al}/T_{Au} is plotted at a velocity which is the average of the velocity corresponding to R_{Al} and that corresponding to RR_{Al}. The range-velocity relationships presented in the next section were used (Eq. (8) and Fig. 14).

For all products the ratio $(\Delta V/\Delta R)_{Au}/(\Delta V/\Delta R)_{Al}$ appears to show similar behavior. In those cases (Sr^{89}, Cd^{115}, Ba^{140}) in which three measurements were made there is a minimum in $(\Delta V/\Delta R)_{Au}/(\Delta V/\Delta R)_{Al}$ at a velocity of about 0.6 $(Mev/nucleon)^{1/2}$.

A comparison of these measurements with theory requires a detailed treatment of electronic stopping at low velocities. Also required is a knowledge of nuclear stopping for cases in which the mass of the stopping atoms is somewhat greater than the mass of the recoils. We are unaware of a theory that adequately treats these aspects of the stopping process.

RANGE-ENERGY CURVES

Energy-loss measurements[13,14] have been made for the median light and median heavy fission products from thermal-neutron-induced fission of U^{235}. The masses of the median light and median heavy products (94.7 and 138.8) were obtained from the initial velocities and the relationships $V_H/V_L = M_L/M_H$ and $M_L + M_H = 233.5$. Ranges in Al and Au for products of these masses were taken from the smooth curves shown in Figs. 3 and 4. Also the corresponding ranges in air can be obtained from Reference 11. The range values for Pu^{239} fission products in air must be corrected for the small difference in kinetic energy[12] of the products from the fission of Pu^{239} and U^{235}.

The energy-loss or velocity-loss measurements have been normalized to the total range values, and the results are summarized in Table VII and Figs. 7-10. The first two columns in Table VII give the energy and corresponding velocity of the median light and heavy products; the next two columns the absorber thickness and corresponding residual range.

The radiochemical measurements of T_{Au} and RR_{Al} have been used to estimate ranges in Au and the corresponding velocities. These estimates were made as follows. For each measurement of F_{Au+Al} the quantities RR_{Al}/R_{Al} and T_{Au}/R_{Au} were calculated and plotted in Fig. 11 against the mass of the fission product. From this graph we have interpolated to the median light and heavy fission products. Thus we have determined values of a thickness of Au that corresponds to a certain residual range in Al. The velocity corresponding to this residual range in Al has been estimated from the range-velocity data in Al as given in the first part of Table VII and in Fig. 7. Figures 7-9 show the range in Al, air, and Au as a function of velocity. Figure 7 also shows that the range-velocity information for Al from Table VI is consistent with measurements of another type, the range of Tb^{149} from nuclear reactions induced by heavy ions.[22] For Al and air an equation of the form

$$R = k V - \Delta \tag{8}$$

(where k and Δ depend on both the fission product and the stopping material) can fit the results rather accurately over quite a wide range. For Au this equation appears to give a fit that is more limited, but the data scatter considerably.

Figure 10 shows log R plotted as a function of log E for median light and heavy products. The smooth curves were simply drawn by eye. An equation of the form

$$R = K E^{\alpha} \tag{9}$$

Table VII. Range-energy data for median light and median heavy fission products

Median light product, A = 94.7					Median heavy product, A = 138.8				
Energy (Mev)	Velocity (Mev per nucleon)$^{\frac{1}{2}}$	Absorber (mg/cm^2)	Residual range (mg/cm^2)	Ref.	Energy (Mev)	Velocity (Mev per nucleon)$^{\frac{1}{2}}$	Absorber (mg/cm^2)	Residual range (mg/cm^2)	Ref.
				Aluminum					
98.7	1.444	0	4.00	a,b	67.5	0.986	0	3.03	a,b
59.8	1.124	1.06	2.94	b	30.0	0.658	1.06	1.97	b
40.4	0.924	1.82	2.18	b	17.6	0.504	1.82	1.21	b
22.3	0.687	2.5	1.5	b					
96.4		0		c	65.6		0		c
				Gold					
98.7	1.444	0	10.4	a,b	67.5	0.986	0	8.0	a,b
62.0	1.144	3.29	7.1	b	33.5	0.695	3.29	4.7	b
37.4	0.889	5.15	5.4	b	19.2	0.526	5.15	2.9	b
79.	1.29	0.61	9.8	d	57.5	0.91	0.61	7.4	d
57.	1.10	2.20	8.2	d	38.5	0.74	2.20	5.8	d
41.	0.93	3.80	6.6	d	27.5	0.63	3.80	4.2	d
17.	0.60	8.35	2.1	d	36.0	0.72	2.5	5.5	e
53.2	1.06	3.3	7.1	e	15.3	0.47	5.5	2.5	e
21.9	0.68	6.9	3.5	e					
6.13	0.36	9.4	1.0	f					
				Air					
98.7	1.444	0	3.02	g,d	67.5	0.986	0	2.29	g,d
93.2	1.40	0.142	2.88	d	60.5	0.93	0.142	2.15	d
84.8	1.34	0.284	2.74	d	54.	0.88	0.284	2.01	d
73.6	1.25	0.556	2.46	d	45.	0.80	0.556	1.73	d
59.	1.12	0.899	2.12	d	33.	0.69	0.899	1.39	d
49.	1.02	1.19	1.83	d	25.	0.60	1.19	1.10	d
42.	0.94	1.37	1.65	d	20.	0.54	1.37	0.92	d
32.	0.82	1.71	1.31	d					
22.	0.68	2.16	0.86	d					

[a] See Figs. 3 and 4. [b] Reference 13. [c] Reference 12. [d] Reference 14.
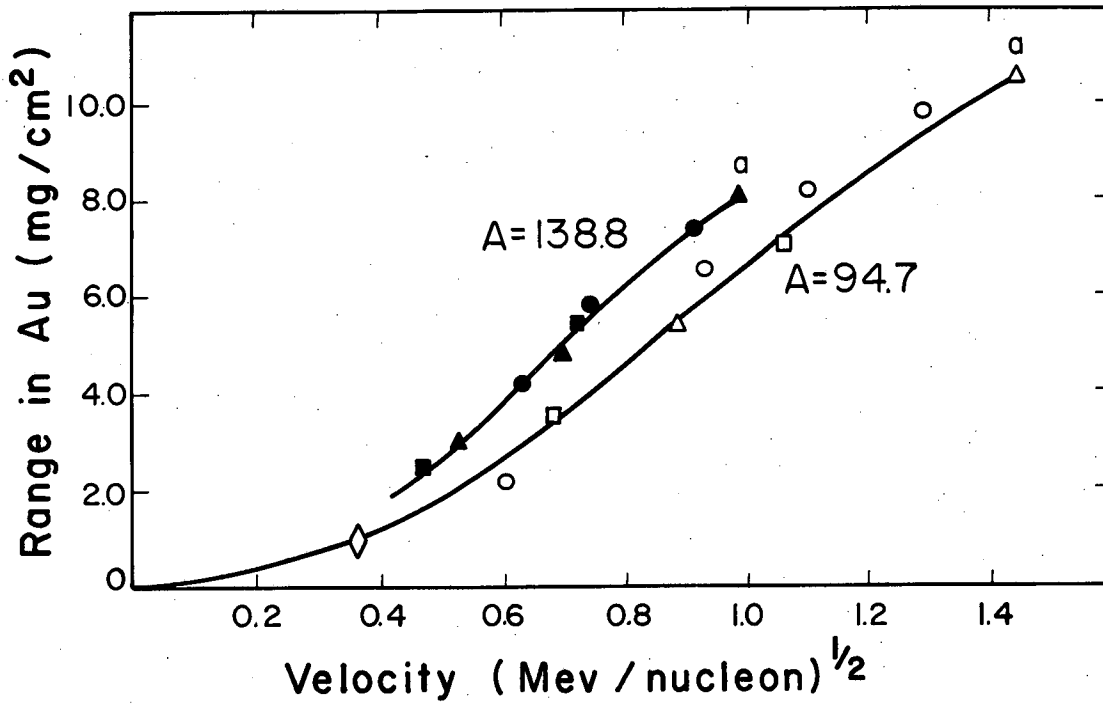[e] This work (see Fig. 7 and 11). [f] Reference 15. [g] Reference 11.
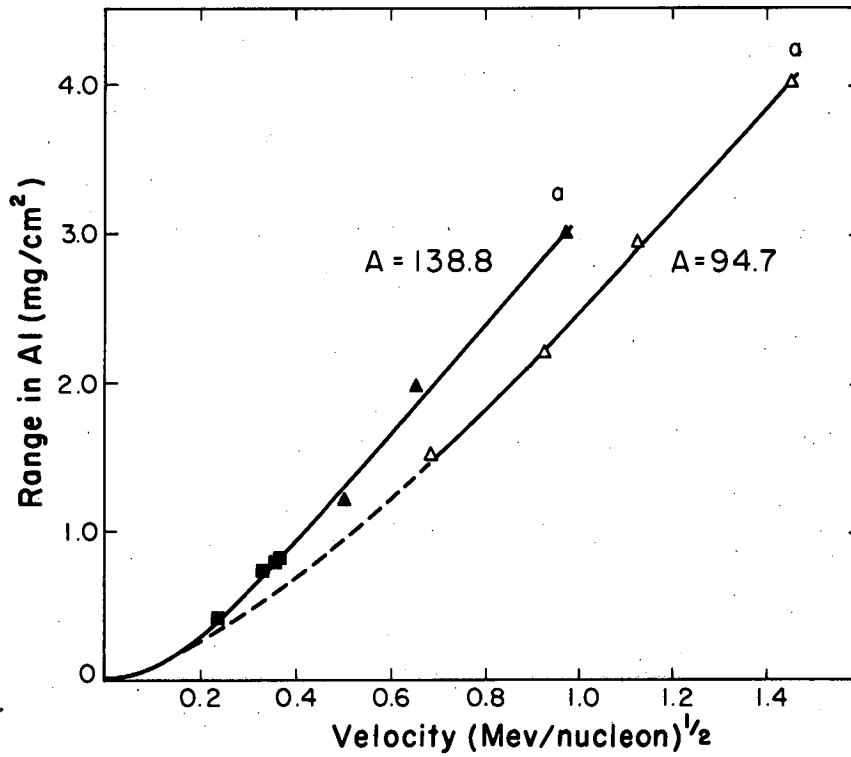
MU—19560

Fig. 7. Range-velocity curve in Al for the median light
(open points) and heavy (closed points) fission
products. The range for points designated by a
is from this work. The initial velocity and
velocity-loss data are from reference 13. The
squares are from the measured range of Tb^{149}
recoils (formed in nuclear reactions, reference
22) converted to the median heavy fragment of the
same velocity.
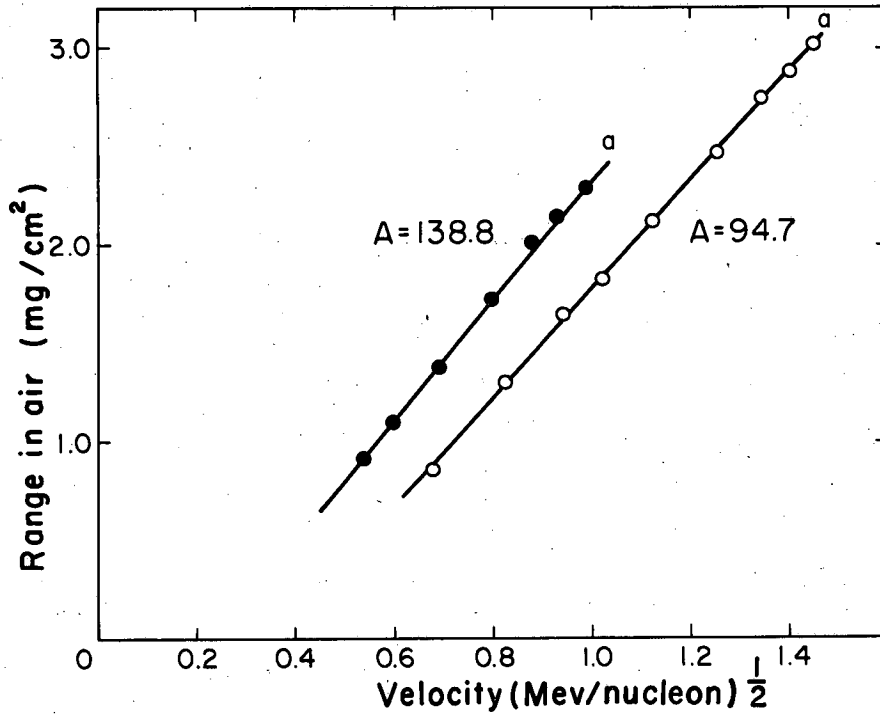
MU-19561

Fig. 8. Range-velocity curves in air for the median light (open points) and heavy (closed points) fission products. The range for points designated by a is from reference 11 (corrected from Pu[239] to U[235] fission). The velocity-loss data are from reference 14.

MU-19562

Fig. 9.　Range-velocity curves in Au for the median light
　　　(open points) and heavy (closed points) fission
　　　products.　The squares are from this work (Fig. 11
　　　and Fig. 7), the triangles from reference 13, the
　　　circles from reference 14, and the diamond from
　　　reference 15 and Fig. 7.　The range for the points
　　　designated by　a　is from this work.
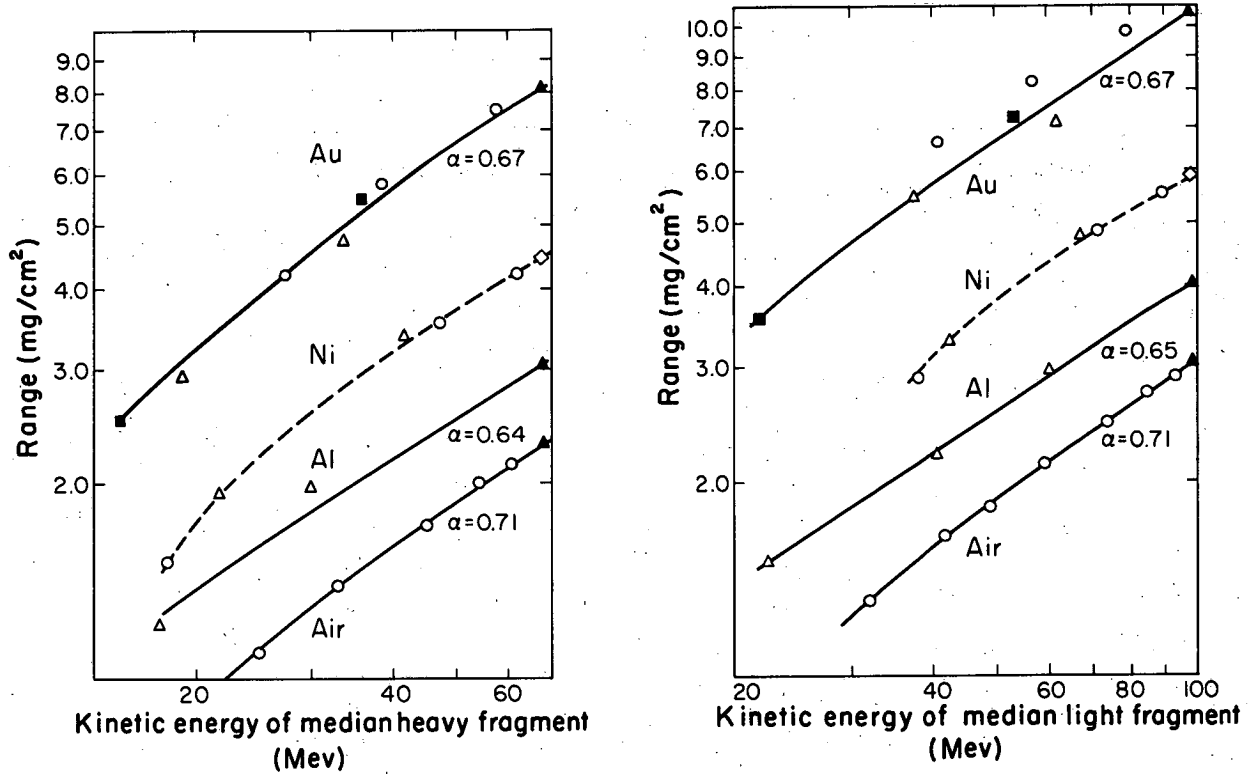
Fig. 10. Log range-log energy curves for the median heavy
    fission product A and median light product B. The
    smooth curves were drawn by eye. A function of the
    form R=KE$^\alpha$ gives an adequate fit for the initial part
    of the range with the indicated value of α. Closed
    points are from radiochemical measurements of the
    range. Open circles are from reference 14; triangles
    are from reference 13. The total range in Ni (◊)
    was estimated in a crude way as described in the
    text. Thus the curve for Ni (---) should be taken
    as only a rough approximation.
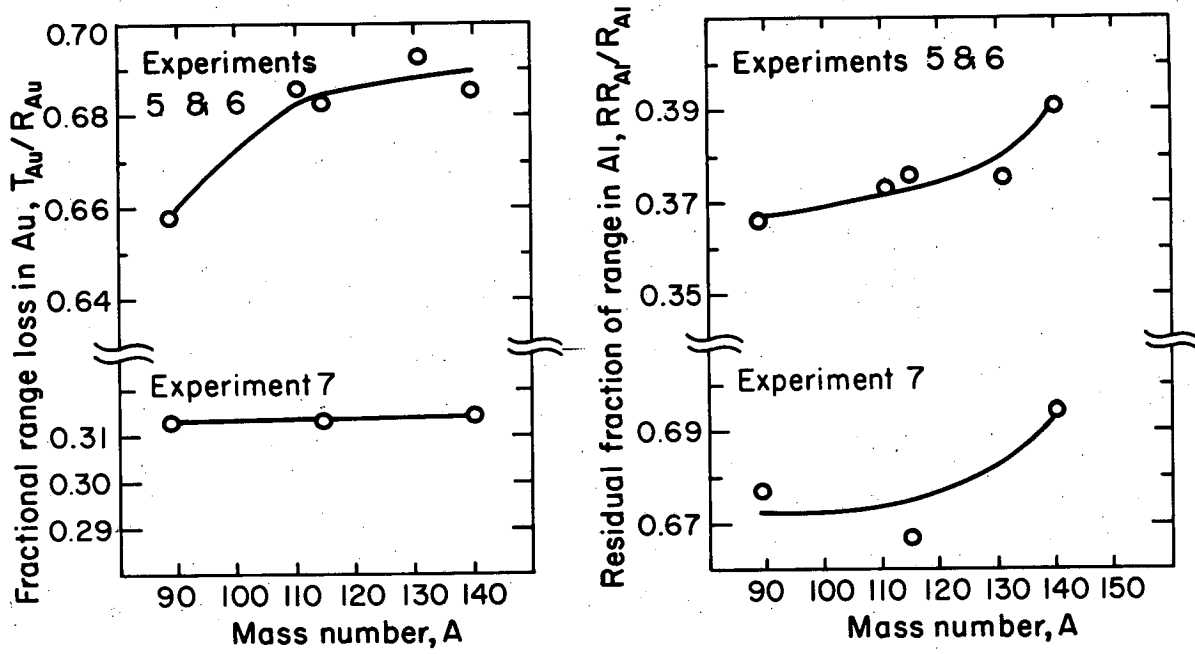
MU – 19565

Fig. 11. Fractional range loss in Au (T_{Au}/R_{Au}) and
fractional residual range in Al(RR_{Al}/R_{Al}).

(where K and α depend on both the fission product and the stopping material) can

given an adequate fit from the initial energy to about one-half the initial

energy. The value of α is in every case about 2/3. The total range in Ni was

crudely estimated with the assumption that $R/M^{1/2}$ is constant (M is the atomic

weight of the stopping material).

There are rather large discrepancies in the energy-loss measurements for

the light fragment in Au, as shown in Figs. 9 and 10. Our measurements and

those by Fulmer[14] were both calibrated by comparison to the energy-loss data in

Al from Leachman and Schmitt.[13] The agreement between the radiochemical

measurements and Fulmer's is satisfactory for the heavy fragment, but rather

poor for the light fragment. We consider the radiochemical measurements to be

more accurate and have thus weighted them more heavily in drawing the smooth

curves in Figs. 9 and 10. Also, a smaller discrepancy exists between the radio-

chemical results and time-of-flight measurements for 3.29 mg/cm^2 Au absorber

(the triangles which correspond to a range of 7.1 mg/cm^2 Au for the light

fragment and 4.7 mg/cm^2 Au for the heavy fragment). The radiochemical results

indicate that the range-energy curves in Al and Au are very nearly proportional

to each other for the initial part of the range, but the proportionality does

not hold at low velocities (see Fig. 5).)

Estimation of Kinetic Energies from Range Measurements

Range measurements which employ radiochemical techniques enable the experi-

menter to make observations with excellent mass resolution. This is a very

important feature when one is interested in the properties of products with very

low yield. In Fig. 3 it is seen that range measurements from U^{235} fission have

been made in Al for the products Ag^{111} and Cd^{115}, for which there is no direct measurement of the kinetic energy. Similarly for Pu^{239}, range data are available for the products Br^{83}, Pd^{112}, In^{117}, and Eu^{157}, for which no kinetic energy measurements have been made.[11] In Fig. 12 the kinetic energy measurements for Pu^{239} fission[12] are shown along with the range data.[11] The similarity of the dependence of range and energy on mass as seen in Figs. 3 and 12 are indicative of a regular dependence of the range-energy relationships on the mass of the fission product.

We assume that Eqs. (8) and (9) may be generalized to all fission products. Each of these equations has two parameters. We have estimated one parameter from the range-energy curves for the median light and heavy products. The other parameter was determined from the total range and the initial energy measurements. The values of k were assumed to be linear functions of mass and were interpolated from the median light and heavy products. Then, the Δ values were calculated from the ranges in Fig. 3 and the initial energies.[12] Similarly, α was taken to be 2/3 in every case and K was calculated. The parameters Δ and K are shown as a function of mass in Figs. 13-15. If we assume that these parameters are smooth functions of mass we can extrapolate and interpolate to the regions of low fission yields. Thus from the range measurements we can estimate kinetic energies. Energy estimates from the two functional forms (Eqs. (8) and (9)) agree to about 0.5 Mev except for Br^{83} in the fission of Pu^{239}. In this case a kinetic energy of 105 Mev was estimated from Eq. (9) and 110 Mev from Eq. (8). This difference reflects uncertainty in the extrapolation of the range-energy parameters.

The energies are shown in Fig. 16 as a function of mass for fission of U^{235} and Pu^{239}. As was proposed by Katcoff, Miskel, and Stanley[11] there appears to
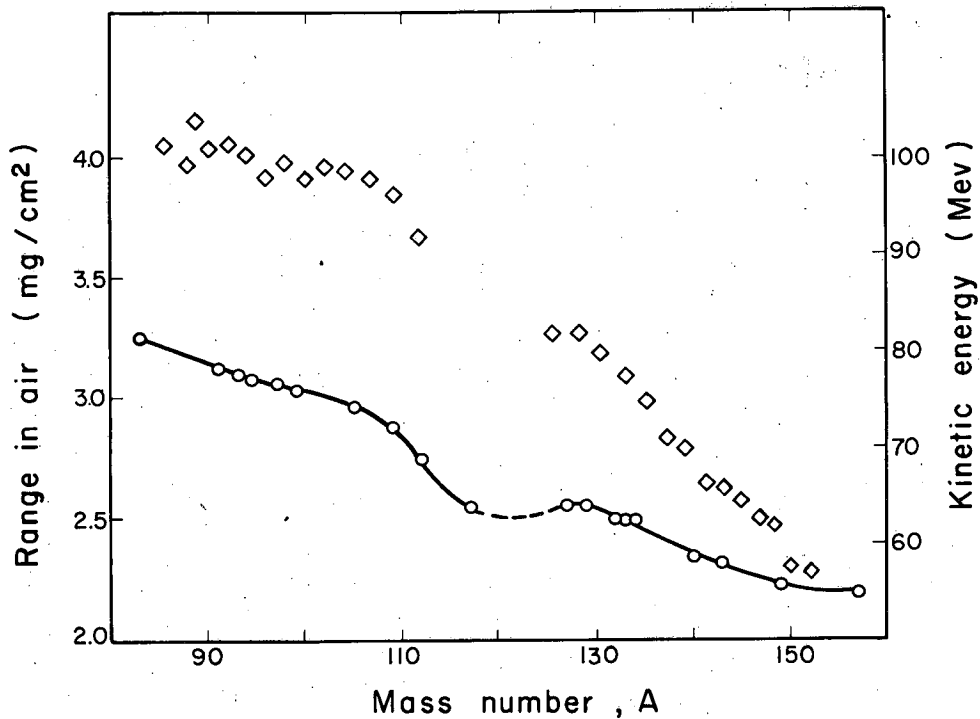
Fig. 12. Range in air and kinetic energy of products
from fission of Pu^{239} induced by thermal-neutron
irradiation. The range measurements O are from
reference 11 and the kinetic energy measurements
◊ are from reference 12.
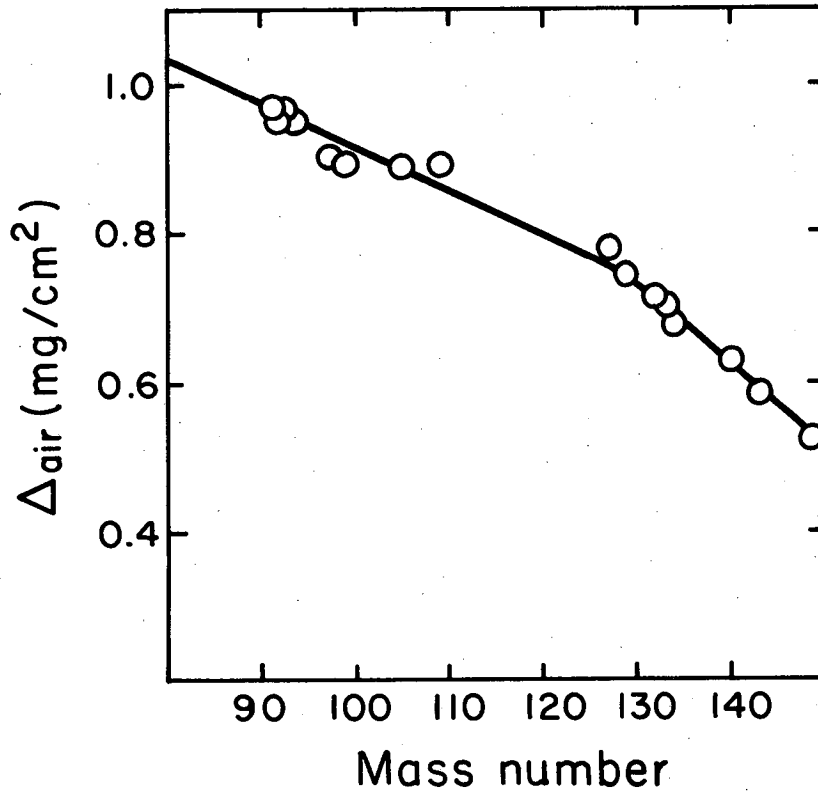
MU-18685
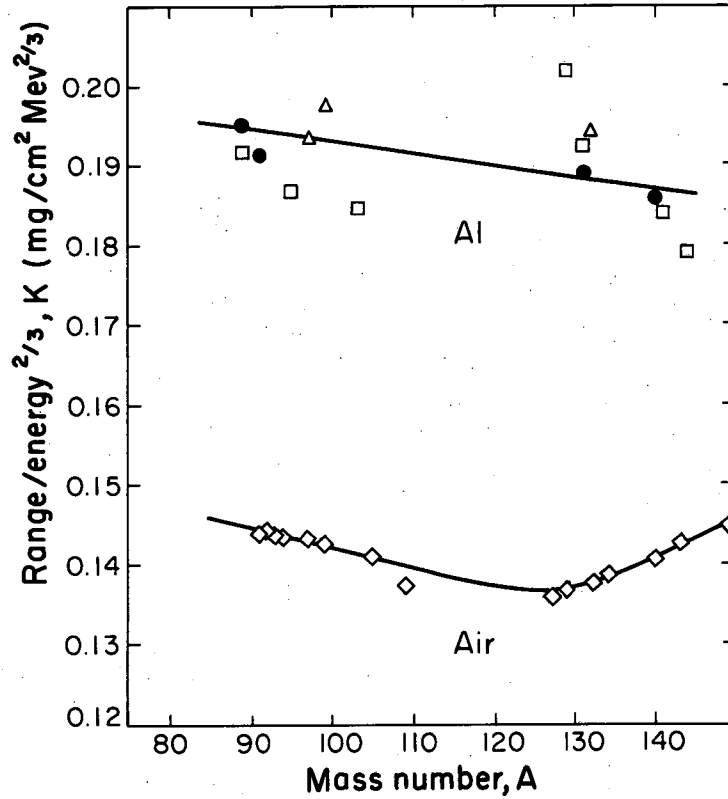
Fig. 13.   The constant Δ_{air} in the relation $R_{air} = k_{air}$
         $V - \Delta_{air}$ calculated from the initial energy (reference
         12) and the total range (reference 11). The value
         of k_{air} was taken to be 5.44×10^{-3} A+2.253 [velocity
         in units of $(Mev/nucleon)^{1/2}$ and range in mg/cm^2 air].
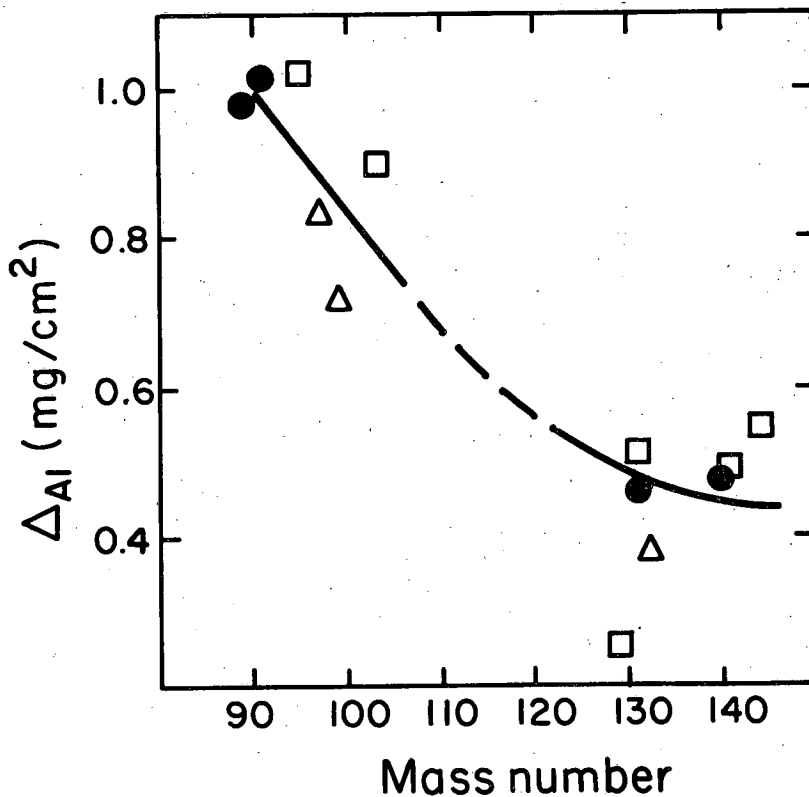
MU-18684

Fig. 14.   The constant Δ_{Al} in the relation $R_{Al} = k_{Al} V - \Delta_{Al}$
calculated from the initial energy (reference 12)
and the total range. The value of k_{Al} was taken to
be $2.84 \times 10^{-3} A + 3.206$ [velocity in units of (Mev/
nucleon)$^{1/2}$ and range in mg/cm^2 Al]. ● Range values
from this work. △ Range values from reference 15.
◻ Range values from reference 16 normalized to
this work.

MU – 19568

Fig. 15. The constant K in the relation R=K E$^{2/3}$, cal-
culated from the initial energy in Mev (reference
12) and the total range (in mg/cm^2). ● Range data
from this work. ☐ Range data from reference 16
normalized to this work. △ Range data from reference
15. ◇ Range data from reference 11.
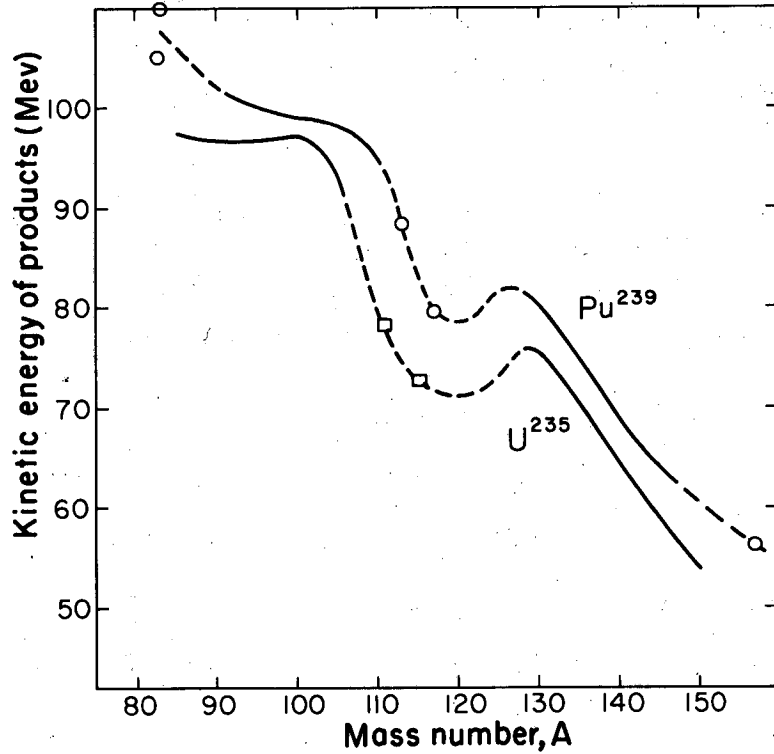
MU – 19569

Fig. 16. The kinetic energy of the fission products.
The solid curves are taken from reference 12, and
the points from range measurements and Eqs. (8) and
(9). The circles are for Pu^{239} fission and were
obtained from range measurements of reference 11.
The squares are for U^{235} and were obtained from
range measurements of this work.

be less kinetic energy released in symmetric fission than in slightly asymmetric

fission. The sum of the kinetic energies of the symmetric products is about

30 Mev less than that of the slightly asymmetric products for fission of U^{235},

and about 20 Mev less for Pu^{239}. This effect may be the result of an irregular-

ity in the range-energy parameters, but we consider it unlikely that there is

an irregularity of this magnitude. This kinetic-energy deficit must be made

up by unusually high excitation energies for the symmetric fragments or by the

emission of particles or photons at the instant of fission.

It is possible that α particles emitted in fission may give rise to this

kinetic energy deficit for near-symmetric products. Dr. Wladyslaw Swiatecki

has made some very interesting observations on this subject, and the ideas in

the discussion of this point are essentially due to him. The yield of α

particles in thermal-neutron-induced fission of U^{235} is about 0.3% as compared

with a fission yield of about 0.01% for a typical product of symmetric fission,

say Cd^{115}. From Fig. 16 it appears that a deficit in kinetic energy of the

products is present over a region of about 30 mass numbers for U^{235} and about 20

mass numbers for Pu^{239}. The kinetic energy spectrum of α particles in fission

has a most probable energy of about 15 Mev, and the separation energy for an α

particle from a symmetric fission fragment would be expected to be about 7 Mev.[24]

Thus if α-particle emission is to completely explain the 20- to 30-Mev kinetic

energy deficit of the near-symmetric fission products, α emission must accompany

almost every symmetric fission event. For slightly asymmetric fission the fission

yields increase very rapidly and the probability for α emission must decrease.

A correlation of the photographic-emulsion measurements of track length in

those events accompanied by α emission[25] has been prepared by Dr. Swiatecki as
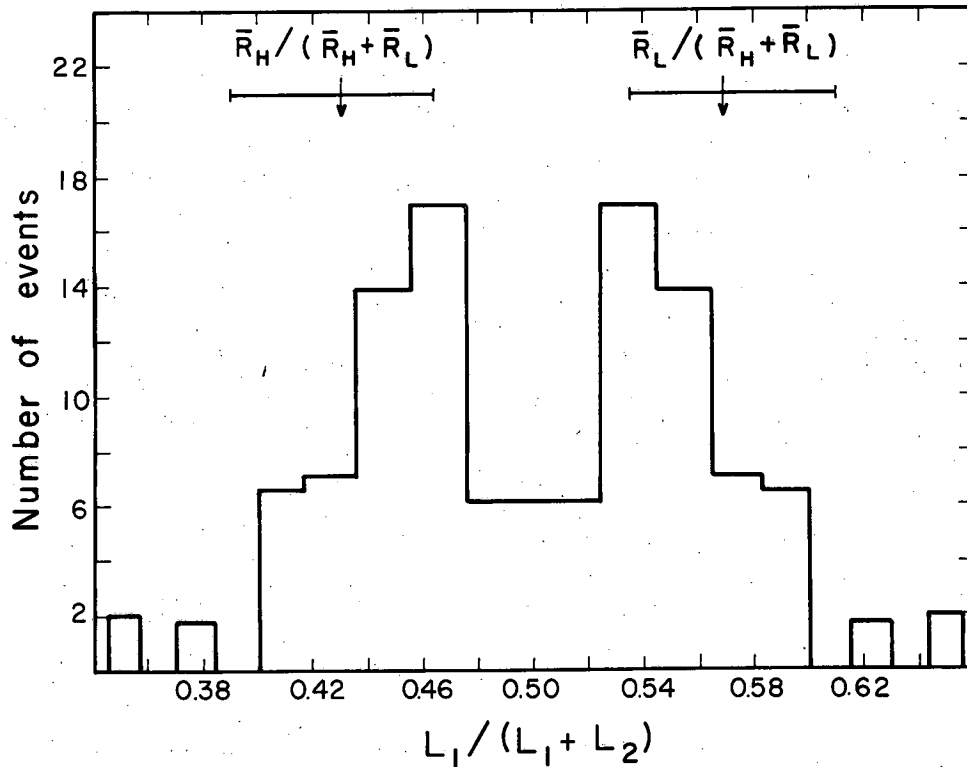
MU-19570

Fig. 17. Correlation (by Dr. W. Swiatecki) of the
lengths of dense tracks reported in reference 24 from
fission of U^{235} accompanied by α-particle emission.
The abscissa is the ratio of the length of one dense
track, L_1, to the sum of the lengths of the two dense
tracks, L_1+L_2. The arrow corresponds to the range
in Al of the median light or heavy fragment $\bar{R}_L$ or
$\bar{R}_H$ over the sum of the ranges of median light and
heavy fragments $\bar{R}_L + \bar{R}_H$. The bar gives an estimate
of the width at half the maximum of the distribution
of $R_L/(R_L + R_H)$ in U^{235} fission. In this plot symme-
try about $L_1/(L_1+L_2) = 1/2$ is required.

shown in Fig. 17. The number of events is plotted against the ratio of the length of one dense track (L_1) to the sum of the lengths of the two dense tracks (L_1+L_2). In this plot symmetry about an $L_1/(L_1+L_2)$ of 1/2 is required, and each measured event appears twice. If α emission was equally probable for all the fission events the peaks of this histogram should correspond to the track lengths of median light and heavy fission products. The poor resolution of the track-length measurements should result in an excess of $L_1/(L_1+L_2)$ ratios both less than and greater than that corresponding to median light and heavy products. If it is assumed that the track length in emulsion is proportional to the range in Al, the arrow corresponds to the $L_1/(L_1+L_2)$ of median light and heavy fission products. Apparently there is an enhanced probability for tracks of more nearly equal length than the ranges of median light and heavy products. This correlation seems to suggest a high probability of α emission for symmetric fission. If a maximum probability for α emission occurs for symmetric fission, it is not necessary that Fig. 17 show a maximum for $L_1/(L_1+L_2) = 1/2$. The observations in Fig. 17 depend on fission yield as well as probability for α emission.

A similar study of α-particle emission in the spontaneous fission of Cf^{254} has been carried out by Drs. Luis Muga and Stanley G. Thompson (Lawrence Radiation Laboratory) using photographic emulsions. A more complete discussion of all the experiments pertinent to this question is being prepared by these workers.[21]

The experimental information is certainly very meager, and no definite conclusion can be drawn. More detailed experimental investigations of this subject are required to test the validity of these suggestions.

APPENDIX

The equations used to analyze the experimental observations are presented in this section. First we derive a simple relationship, Eq. (1), for calculating the range from experiments in which the catcher foils are of the same material. Then we consider the situation in which catcher foils of different materials are used. The different scattering properties of the two materials are included in the derivation of Eqs. (5) and (6).

For fission induced by thermal-neutron irradiation the fissile nucleus is essentially at rest and the angular distribution is isotropic. Thus F_t, the fraction of the activity from a thin target of thickness W that passes through a catcher of thickness t, is given as

$$F_t = \frac{1}{4\pi W} \int_0^W dx \int_0^{\Theta_{max}} 2\pi\sin\Theta\, d\Theta. \tag{10}$$

The symbol x denotes the distance in the fissile target layer of the fission event from the surface of the catcher in question. The angle Θ is defined by the normal to the target layer and the direction of recoil. The limit of integration Θ_{max} is determined by the residual range R' of the product as it emerges from the target layer (see Fig. 18A):

$$\cos\Theta_{max} = t/R'. \tag{11}$$

If the target layer is thin with respect to the range of the product, we may approximate the rate of velocity loss in the target layer $-\frac{dV}{dx}$ as proportional to the rate of velocity loss in the catcher $(\frac{dV}{dR})$:

$$-\frac{dV}{dx} = c\,\frac{dV}{dR}. \tag{2}$$
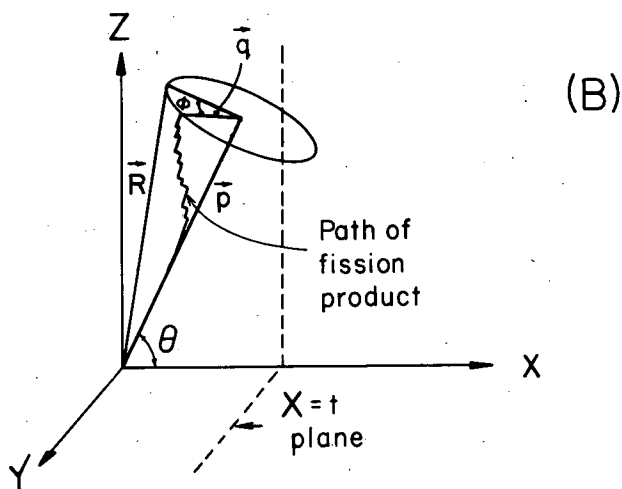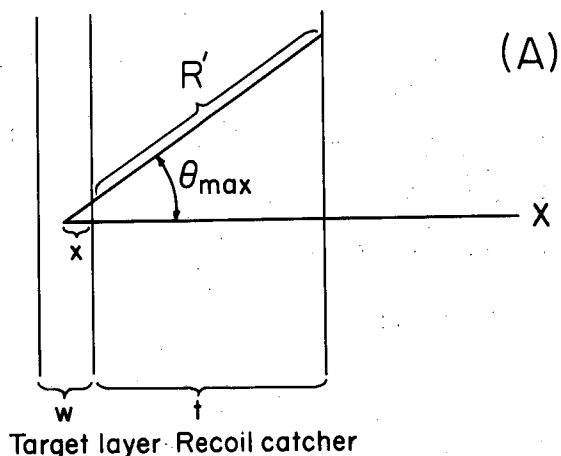
Fig. 18.   Vector diagram of the recoiling fission product.
The X axis is chosen to be normal to the surface of
the target layer.   The X=t plane represents the
interface between catcher 1 and catcher 2.   If all
catcher foils are of the same material, scattering
phenomena need not be considered and the upper dia-
gram (A) is appropriate [see Eqs. (10) and (11)].
      The lower diagram (B) indicates the recoil path
of a particular product from an infinitely thin
fissile layer in the YZ plane.   The Z axis is chosen
to be in the plane defined by the X axis and the
initial recoil direction $\vec{p}$.   The angle φ is defined
by the XZ plane and the component of the range $\vec{q}$
perpendicular to the original recoil path.

The symbol R refers to the range of the product in the material used as a catcher foil.

Now, we have $\cos \Theta_{max} = (t + cx)/R$ (12)

and $F_t = 1/2 \, (1 - t/R - cW/2R),$ (1)

or $F_t = 1/2 \, (1 - t'/R),$ (13)

where $t' = t + cW/2.$ (14)

In this development we have treated R as a unique quantity. It is clear that if there is a distribution of R values the average value of F_t is the observed quantity and the use of Eq. (1) yields the average value of the reciprocal of the range. This statement is correct only if all values of R are greater than $t + cW$ or, for practical purposes, if $R - t - cW$ is greater than the range straggling.

If different materials are used as catcher foils, differences in scattering properties may give rise to deviations from Eq. (1). The foregoing analysis does not take account of angular deflection. We assume that the recoiling product moves straight initially and suffers deflections as it approaches the end of the range, as shown in Fig. 18B. The vector $\vec{p}$ is the average component of range along the original direction of motion and $\vec{q}$ is the average component of the range perpendicular to the original direction of motion. Then we have

$$\vec{R} = \vec{p} + \vec{q} \,,$$ (15)

$$R = (p^2 + q^2)^{1/2} = p[1 + (q/p)^2]^{1/2}.$$ (16)

The vector $\vec{q}$ may be directed with equal probability at all azimuthal angles φ measured with respect to the plane of $\vec{p}$ and the normal to the target layer (X, Z plane in Fig. 18B).

Let us consider an infinitely thin target layer on the **YZ** plane, and let Θ be the angle between $\hat{p}$ and the normal to the **YZ** plane. Then for the fraction F_b' of the recoils that backscatter from one catcher foil we have $\Theta < \pi/2$, but final values of X are negative:

$$F_b' = \frac{1}{4\pi} \int_{-\pi/2}^{\pi/2} d\varphi \int_{\pi/2}^{\Theta_{min}} \sin \Theta d\Theta, \qquad (17)$$

where

$$p \cos \Theta_{min} = q \cos \varphi \sin \Theta_{min}; \qquad (18)$$

after integration,

$$F_b' = \frac{1}{2\pi} \arc \sin \left(\frac{q}{R}\right) \cong \frac{1}{2\pi} \frac{q}{R}. \qquad (19)$$

If the catching materials are identical on either side of the target layer, then the net fraction backscattered, F_b, is zero, but if the materials differ as designated by subscripts, then we have

$$F_b \cong \frac{1}{2\pi} \left[\left(\frac{q}{R}\right)_i - \left(\frac{q}{R}\right)_j \right]. \qquad (8)$$

If we assume that the range-energy relationships in materials i and j are simply proportional to each other, we can derive a relationship for the fraction of the activity, $_jF_i$, that passes through a thickness t_i of material i (with $t > q_i$) into a catcher of material j:

$$_jF_i = \frac{1}{2} - \left(\frac{t}{2p}\right)_i + _jFS_i - _jBS_i. \qquad (20)$$

The symbol $_jFS_i$ denotes the fraction of the recoils that are forescattered from material i into material j, and $_jBS_i$ designates the fraction of the recoils backscattered from material j into material i:

$$_jFS_i = \frac{1}{4\pi} \int_{-\pi/2}^{\pi/2} d\varphi \int_{\cos^{-1}(t/p)_i}^{\Theta_{max}} \sin \Theta \, d\Theta \qquad (21)$$

where $p_i \cos \Theta_{max} + q_i \cos \varphi \sin \Theta_{max} = t_i$. $\hfill (22)$

Thus $_jFS_i = \frac{1}{2\pi} \left(\frac{q}{p}\right)_i \left[1 - \frac{t^2}{2R^2} - \frac{t^4}{8R^4} + \ldots\right]_i + \frac{1}{8} \left(\frac{t}{p}\right)_i \left(\frac{q}{R}\right)_i^2$

$$- \frac{1}{6\pi} \left(\frac{q}{p}\right)_i^3 \left[1 + \ldots\right] + \ldots \hfill (23)$$

In order to obtain $-{}_jBS_i$, Eq. (22) is replaced by

$$(\alpha p_i + \beta p_j) \cos \Theta_{min} - q_j \cos \varphi \sin \Theta_{min} = t_i, \hfill (24)$$

where α is $t_i/p_i \cos \Theta$ and βp_j is the component of the residual range in material j parallel to the original velocity. To a good approximation $(\alpha p_i + \beta p_j)$ can be replaced by p_i because we are concerned only with those recoils which penetrate a very short distance into material j and are then scattered back into material i. Thus $-{}_jBS_i$ can be obtained by replacing q_i in Eq. (23) by $-q_j$:

$$_j{}^{-BS}{}_i = -\frac{1}{2\pi} \left(\frac{q_j}{p_i}\right) \left[1 - \frac{t^2}{2R^2} - \frac{t^4}{8R^4} + \ldots\right]_i + \frac{1}{8} \left(\frac{t}{p}\right)_i \left(\frac{q_j}{R_i}\right)^2 + \frac{1}{6\pi}\left(\frac{q}{p}\right)_1^3 \left[+ \ldots \right] ($$

$$\left[1 + \ldots\right] + \ldots \hfill (24)$$

Now $_jF_i = \frac{1}{2} - \frac{1}{2}\left(\frac{t}{p}\right)_i + \frac{1}{2\pi}\left[\frac{q_i}{R_i} - \frac{q_j}{R_i}\right]\left[1 - \frac{t^2}{2R^2} - \frac{t^4}{8R^4} + \ldots\right]_i$

$$+ \frac{1}{8} \left(\frac{t}{R}\right)_i \left[\left(\frac{q_i}{R_i}\right)^2 + \left(\frac{q_j}{R_i}\right)^2\right] + \ldots \hfill (25)$$

In order to correct for a thin target layer in Eqs. (22)-(25), t is replaced by t' from Eq. (14). If $q_i = q_j$ Eq. (25) reduces to Eq. (1), and if $q_i \gg q_j$, then Eq. (25) reduces to Eq. (6).

ACKNOWLEDGEMENTS

REFERENCES

1. E. M. Douthett and D. H. Templeton, Phys. Rev. 94, 128 (1954).

2. Nathan Sugarman, Milton Compos, and Karoline Wielgoz, Phys. Rev. 101, 388 (1956).

3. Norbert T. Porile and Nathan Sugarman, Phys. Rev. 107, 1410 (1957); Norbert T. Porile, Phys. Rev. 108, 1526 (1957).

4. Christiane Baltzinger, Yield and Range Studies of Selected Fission Products from Uranium Bombarded with Bev Protons, Lawrence Radiation Laboratory Report UCRL-8430, Aug. 1958.

5. Cohen, Jones, McCormick, and Ferrell, Phys. Rev. 94, 625 (1954).

6. Cohen, Ferrell-Bryan, Coombe, and Hullings, Phys. Rev. 98, 685 (1955).

7. E. J. Winhold and I. Halpern, Phys. Rev. 103, 990 (1956).

8. C. T. Coffin and I. Halpern, Phys. Rev. 112, 536 (1958).

9. J. W. Meadows, Phys. Rev. 110, 1109 (1958).

10. R. Wolke and J. Gutmann, Phys. Rev. 107, 850 (1957).

11. Katcoff, Miskel, and Stanley, Phys. Rev. 74, 631 (1948).

12. William E. Stein, Phys. Rev. 108, 94 (1957).

13. R. B. Leachman and H. W. Schmitt, Phys. Rev. 96, 1366 (1954).

14. Clyde B. Fulmer, Phys. Rev. 108, 1113 (1957), and "Fission Fragment Studies by Magnetic Analysis," Oak Ridge National Laboratory Report ORNL-2320, Aug. 1957.

15. P. F. Suzor, Ann. Phys. 4, 269 (1949).

16. Finkle, Hoagland, Katcoff, and Sugarman, in "Radio-Chemical Studies: The Fission Products," National Nuclear Energy Series (McGraw-Hill Book Co., Inc., New York, 1951), Div. IV, Vol. 9, p. 471.

17. Albert Ghiorso and Torbjørn Sikkeland, in Proceedings of the Second United Nations International Conference on the Peaceful Uses of Atomic Energy, Geneva, 1958, (United Nations, New York, 1959), Vol. 14, P/2440, p. 158.

18. Radio-Chemical Studies: The Fission Products, National Nuclear Energy Series, (McGraw-Hill Book Co., Inc., New York, 1951), Div. IV, Vol. 9.

19. N. Bohr, Kgl. Danske Videnskab. Selskab. Mat.-fys. Medd. 18, No. 8 (1948).

20. Luis Muga (Lawrence Radiation Laboratory), private communication, 1959.

21. Bøggild, Arrøe, and Sigurgeirsson, Phys. Rev. 71, 281 (1947).

22. Lester Winsberg and J. M. Alexander, "The Stopping of Heavy Atoms," to be submitted to Phys. Rev.

23. A. G. W. Cameron, A Revised Semi-Empirical Atomic Mass Formula, Atomic Energy of Canada Limited Report CRP-690, 1957.

24. L. Marshall, Phys. Rev. 75, 1339 (1949).